5912 *Organometallics* **2010,** *29,* 5912–5918
DOI: 10.1021/om1007133

ORGANOMETALLICS
Article

Fully Delocalized (Ethynyl)(vinyl)phenylene-Bridged Diruthenium Radical Complexes

Florian Pevny,[†,‡] Emmanuel Di Piazza,[§] Lucie Norel,[§] Malte Drescher,[‡] Rainer F. Winter,*[,†,‡] and Stéphane Rigaut*[,§]

[†]*Institut für Anorganische Chemie der Universität Regensburg, Universitätsstrasse 31, D-93040 Regensburg, Germany,* [‡]*Fachbereich Chemie der Universität Konstanz, Universitätsstrasse 10, D-78453 Konstanz, Germany, and* [§]*UMR 6226 CNRS-Université de Rennes 1, Sciences Chimiques de Rennes, Campus de Beaulieu, F-35042, Rennes Cedex, France*

Received July 20, 2010

Diruthenium complexes $(X)(dppe)_2Ru-C\equiv C-1,4\text{-}C_6H_4-CH=CH-RuCl(CO)(P^iPr_3)_2$ (X = Cl, **1a**; X = C≡CPh, **1b**) containing an unsymmetrical (ethynyl)(vinyl)phenylene bridging ligand are compared to their symmetrical 1,4-bis(ethynyl)phenylene- and 1,4-divinylphenylene-bridged congeners and their mononuclear alkynyl precursors. Electrochemical and UV/vis/NIR, IR, and EPR spectroscopic studies on the neutral complexes and their various oxidized forms indicate bridging ligand-centered oxidation processes and uniform charge and spin delocalization over both dislike organoruthenium moieties despite differences in their intrinsic redox potentials. Comparison between the chloro and the phenylacetylide-terminated derivatives **1a**,**b** suggests further that the conjugated organometallic π-system extends over the entire unsaturated backbone including the terminal ligand at the alkynyl ruthenium site. This paves the way to even more extended π-conjugated organoruthenium arrays for long-range electronic interactions.

Introduction

Within the field of organometallic "mixed-valent" chemistry, 1,4-diethynylphenylene has gained particular popularity as a bridging ligand because of the ready availability of the parent alkyne, its good ability to electronically couple the bridged sites, and the stability it conveys to the oxidized forms. At the same time, the 1,4-diethynylphenylene ligand has turned out as an excellent example of Janus-headed behavior with respect to Jørgensen's original definition of a noninnocent ligand. According to that definition, a ligand is called noninnocent if it does not allow the oxidation state of the metal to be defined.[1] This is well illustrated by the comparison of diiron[2−8] and diruthenium[7,9−13] 1,4-diethynylphenylene-bridged complexes. Mostly metal-based oxidation processes in the diiron systems contrast with bridging ligand-dominated oxidations in the diruthenium ones. Thus, while the "classical" description of a bridging ligand allowing for electron exchange between the reduced and oxidized termini in mixed-valent states may be adequate for most iron systems, this is clearly not the case for their ruthenium counterparts. The underlying reason is the lower energy of the Ru 4d compared to the Fe 3d orbitals and the higher ligand character of the highest occupied molecular orbital (HOMO) resulting from the overlap of the metal dπ- and the appropriate π-orbital of the carbon-rich bridging ligand.

By far the majority of all systems investigated to date feature two identical sets of metal atoms and co-ligands as the termini. Complexes with two different metal end groups include some ruthenium−palladium,[14] rhenium−platinum,[15] iron−rhenium,[16,17] and iron−ruthenium[18] derivatives. In most of

*To whom correspondence should be addressed. E-mail: rainer.winter@uni-konstanz.de.

(1) Jørgensen, C. K. *Coord. Chem. Rev.* **1966**, *1*, 164–178.
(2) Le Narvor, N.; Lapinte, C. *Organometallics* **1995**, *14*, 634–639.
(3) Weyland, T.; Ledoux, I.; Brasselet, S.; Zyss, J.; Lapinte, C. *Organometallics* **2000**, *19*, 5235–5237.
(4) Ibn Ghazala, S.; Paul, F.; Toupet, L.; Roisnel, T.; Hapiot, P.; Lapinte, C. *J. Am. Chem. Soc.* **2006**, *128*, 2463–2476.
(5) Tanaka, Y.; Shaw-Taberlet, J. A.; Justaud, F.; Cador, O.; Roisnel, T.; Akita, M.; Hamon, J.-R.; Lapinte, C. *Organometallics* **2009**, *28*, 4656–4669.
(6) Field, L. D.; George, A. V.; Laschi, F.; Malouf, E. Y.; Zanello, P. *J. Organomet. Chem.* **1992**, *435*, 347–356.
(7) Colbert, M. C. B.; Lewis, J.; Long, N. J.; Raithby, P. R.; Younus, M.; White, A. J. P.; Williams, D. J.; Payne, N. N.; Yellowlees, L.; Beljonne, D.; Chawdhury, N.; Friend, R. H. *Organometallics* **1998**, *17*, 3034–3043.
(8) Medei, L.; Orian, L.; Semeikin, O. V.; Peterleitner, M. G.; Ustynyuk, N. A.; Santi, S.; Durante, C.; Ricci, A.; Lo Sterzo, C. *Eur. J. Inorg. Chem.* **2006**, 2582–2597.
(9) Klein, A.; Lavastre, O.; Fiedler, J. *Organometallics* **2006**, *25*, 635–643.
(10) Gao, L.-B.; Kan, J.; Fan, Y.; Zhang, L.-Y.; Liu, S.-H.; Chen, Z.-N. *Inorg. Chem.* **2007**, *46*, 5651–5664.
(11) Armitt, D. J.; Bruce, M. I.; Gaudio, M.; Zaitseva, N. N.; Skelton, B. W.; White, A. H.; Le Guennic, B.; Halet, J.-F.; Fox, M. A.; Roberts, R. L.; Hartl, F.; Low, P. J. *Dalton Trans.* **2008**, 6763–6775.
(12) Olivier, C.; Kim, B.; Touchard, D.; Rigaut, S. *Organometallics* **2008**, *27*, 509–518.
(13) Fox, M. A.; Farmer, J. D.; Roberts, R. L.; Humphrey, M. G.; Low, P. J. *Organometallics* **2009**, *28*, 5266–5269.
(14) Lavastre, O.; Plass, J.; Bachmann, P.; Guesmi, S.; Moinet, C.; Dixneuf, P. H. *Organometallics* **1997**, *16*, 184–189.
(15) Lam, S. C.-F.; Yam, V. W.-W.; Wong, K. M.-C.; Cheng, E. C.-C.; Zhu, N. *Organometallics* **2005**, *24*, 4298–4305.
(16) Wong, K. M.-C.; Lam, S. C.-F.; Ko, C.-C.; Zhu, N.; Yam, V. W.-W.; Roué, S.; Lapinte, C.; Fathallah, S.; Costuas, K.; Kahlal, S.; Halet, J.-F. *Inorg. Chem.* **2003**, *42*, 7086–7097.

Published on Web 10/15/2010

Scheme 1

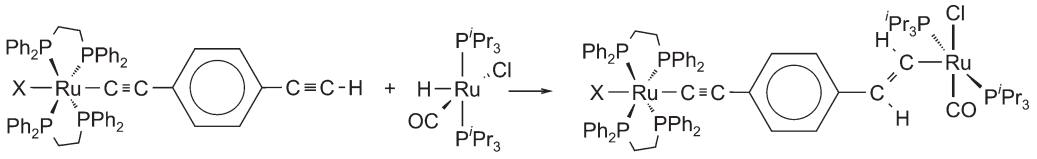

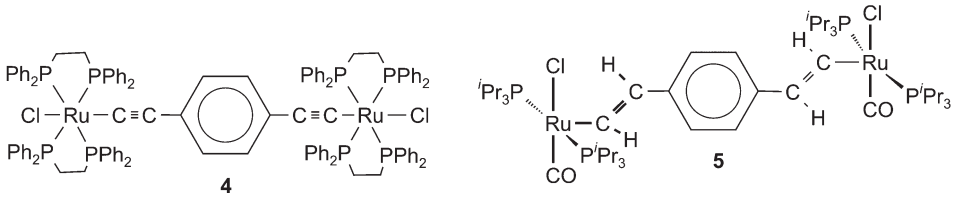

these cases the two dislike metal moieties differ grossly in their electronic properties. As a consequence of such redox asymmetry, their mixed-valent radical cations arising from one-electron oxidation display charge and spin localization on the more electron-rich metal−alkynyl site. Notable exceptions are the iron−ruthenium complexes Cp*(dppe)Fe−C≡C−1,4-C_6H_4−C≡C−Ru(dppe)$_2$Cl and Cp*(dppe)Fe−C≡C−1,4-C_6H_4−C≡C−Ru(dppe)$_2$(C≡C−1,4-$C_6H_4NO_2$) (Cp* = η^5-C_5Me_5; dppe = 1,2-bis(diphenylphosphino)ethane, $Ph_2PC_2H_4PPh_2$), where sizable electronic couplings of ca. 1100 cm^{-1} have been deduced from the Hush-type analysis of their intervalence charge-transfer (IVCT) bands.[18] This is to be contrasted to a value of just 30 cm^{-1} in the iron−rhenium complex Cp*(dppe)Fe−C≡C−1,4-C_6H_4−C≡C−Re(bipy)(CO)$_3$Cl (bipy = 2,2′-bipyridine).[16]

Divinylphenylene-bridged diiron[19] and diruthenium[20−25] complexes strongly resemble their diethynylphenylene-bridged counterparts. Thus, some of us have described bridge-dominated redox processes of 1,4-divinylphenylene-bridged diruthenium complexes {(4-EtOOCpy)(PPh$_3$)$_2$(CO)ClRu}$_2$-(μ-CH=CH-1,4-C_6H_4−CH=CH) and {(P^{i}Pr$_3$)$_2$(CO)ClRu}$_2$-(μ-CH=CH-1,4-C_6H_4−CH=CH).[22−24] Spectroscopic investigations on their radical cations utilizing the charge-sensitive Ru(CO) IR marker band and the resolved hyperfine splitting patterns in the EPR spectrum disclosed full electron and spin delocalization (or nearly so) over both vinyl ruthenium entities. Given the rather similar properties of the diethynylphenylene and the divinylphenylene bridging ligands and of the (X)(dppe)$_2$Ru−C≡C and the (P^{i}Pr$_3$)$_2$(CO)ClRu−CH=CH moieties, it seemed of interest to prepare and investigate unsymmetrical complexes that blend both these motifs into a single system. Making use of the various spectroscopic labels they offer allows us to address the degree of electron delocalization at their various oxidation states, as has just successfully been demonstrated for a vinyl-bridged ruthenium−ferrocene system.[26] Herein we report our findings on (X)(dppe)$_2$Ru−C≡C−1,4-C_6H_4−CH=CH−RuCl(CO)(P^{i}Pr$_3$)$_2$ (X = Cl, **1a**; X = C≡CPh, **1b**) and their alkynyl precursors (X)(dppe)$_2$Ru−C≡C−1,4-C_6H_4−C≡C−R (R = H, **2a**,**b**; R = SiMe$_3$, **3a**,**b**) en route to still larger systems with enhanced conjugation over long path lengths and increased ligand participation to the "redox orbitals".

Results and Discussion

The synthesis of complexes **1a** and **1b** was achieved by combining equimolar amounts of the known alkynyl complexes (X)(dppe)$_2$Ru−C≡C−1,4-C_6H_4−C≡C−H (**2a**, **b**)[12,27] and the hydride ruthenium complex RuClH(CO)-(P^{i}Pr$_3$)$_2$[28] in dichloromethane (Scheme 1). These reactions involve the regio- and stereospecific insertion of a terminal alkyne into the Ru−H bond of the hydride complex and provide 1,2-disubstituted vinyl ligands with a *trans* disposition of the metal atom and the aryl substituent.[28−31] Despite their mechanistic intricacy,[32] alkyne insertions are usually complete within 15 min and afford the unsymmetrically bridged enynyl complexes in >90% yields. The presence of both the ruthenium vinyl and ruthenium ethynyl end groups in **1a**,**b** follows from the observation of the typical Ru−C≡*C* and Ru−CH=CH resonance signals at 113.6 (**1a**) or 117.4 (**1b**) (Ru−C≡*C*), 148.0 (**1a**) or 148.4 (**1b**) (Ru−*C*H), and

(17) Jiao, H.; Costuas, K.; Gladysz, J. A.; Halet, J.-F.; Guillemot, M.; Toupet, L.; Paul, F.; Lapinte, C. *J. Am. Chem. Soc.* **2003**, *125*, 9511–9522.
(18) Gauthier, N.; Olivier, C.; Rigaut, S.; Touchard, D.; Roisnel, T.; Humphrey, M. G.; Paul, F. *Organometallics* **2008**, *27*, 1063–1072.
(19) Field, L. D.; George, A. V.; Malouf, E. Y.; Hambley, T. W.; Turner, P. *Chem. Commun.* **1997**, 133–134.
(20) Wu, X. H.; Jin, S.; Liang, J. H.; Yong, Z.; Yu, G.-a.; Liu, S. H. *Organometallics* **2009**, *28*, 2450–2459.
(21) Seetharaman, S. K.; Chung, M.-C.; Englich, U.; Ruhlandt-Senge, K.; Sponsler, M. B. *Inorg. Chem.* **2007**, *46*, 561–567.
(22) Maurer, J.; Winter, R. F.; Sarkar, B.; Fiedler, J.; Záliš, S. *Chem. Commun.* **2004**, 1900–1901.
(23) Maurer, J.; Sarkar, B.; Kaim, W.; Winter, R. F.; Záliš, S. *Chem.—Eur. J.* **2007**, *13*, 10257–10272.
(24) Maurer, J.; Sarkar, B.; Schwederski, B.; Kaim, W.; Winter, R. F.; Záliš, S. *Organometallics* **2006**, *25*, 3701–3712.
(25) Záliš, S.; Winter, R. F.; Kaim, W. *Coord. Chem. Rev.* **2010**, *254*, 1383–1396.
(26) Kowalski, K.; Linseis, M.; Winter, R. F.; Zabel, M.; Záliš, S.; Kelm, H.; Krüger, H.-J.; Sarkar, B.; Kaim, W. *Organometallics* **2009**, *28*, 4196–4209.
(27) Hurst, S. K.; Cifuentes, M. P.; McDonagh, A. M.; Humphrey, M. G.; Samoc, M.; Luther-Davies, B.; Asselberghs, I.; Persoons, A. *J. Organomet. Chem.* **2002**, *642*, 259–267.
(28) Werner, H.; Esteruelas, M. A.; Otto, H. *Organometallics* **1986**, *5*, 2295.
(29) Werner, H.; Meyer, U.; Peters, K.; von Schnering, H. G. *Chem. Ber.* **1989**, *122*, 2089–2107.
(30) Hill, A. F. In *Comprehensive Organometallic Chemistry II*; Shriver, D. E.; Bruce, M. I., Eds.; Pergamon: Oxford, 1995; Vol. *7*, pp 399−411.
(31) Maurer, J.; Linseis, M.; Sarkar, B.; Schwerderski, B.; Niemeyer, M.; Kaim, W.; Záliš, S.; Anson, C.; Zabel, M.; Winter, R. F. *J. Am. Chem. Soc.* **2008**, *130*, 259–268.
(32) Marchenko, A. V.; Gérard, H.; Eisenstein, O.; Caulton, K. G. *New J. Chem.* **2001**, *25*, 1244–1255.

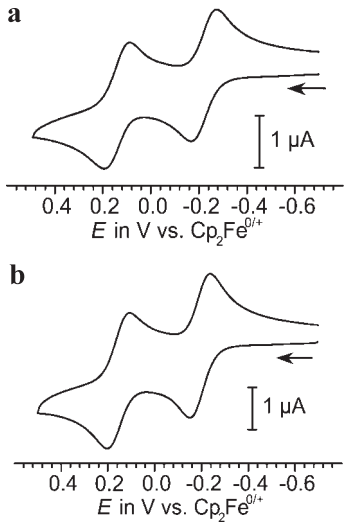

Figure 1. Voltammetric scans of complexes **1a** (upper curve) and **1b** (lower curve) in CH_2Cl_2/NBu_4PF_6 (0.1 M) at rt and v = 0.1 V/s.

134.4 (**1a**) or 134.9 (**1b**) (Ru−CH=*C*H) ppm and of the four resonance signals of an unsymmetrically substituted 1,4-phenylene ring in ^{13}C NMR spectroscopy, from the typical resonance signals of the CH=CH protons of the vinyl group at 8.40 (Ru−C*H*=CH) and 5.95 (Ru−CH=C*H*) ppm and the presence of the phenylene, dppe, and P^{i}Pr$_3$ protons in the correct integral ratios, and from the two sharp singlets at δ = 49.5 (**1a**) or 53.8 (**1b**) (dppe) and 38.5 (P^{i}Pr$_3$) ppm in ^{31}P NMR spectroscopy. The CH=CH ^{13}C NMR values are to be compared to those of the symmetrically substituted {(P^{i}Pr$_3$)$_2$(CO)ClRu}$_2$(μ-CH=CH-1,4-C$_6$H$_4$−CH=CH) (**5**) at δ = 148.5 (Ru-*C*H) and 134.5 (Ru-CH=*C*H) ppm. Complex **1b** also features the C$_\beta$ resonance signal of the phenylacetylide ligand, which was disseminated from that of the bridging ligand by virtue of appropriate HMBC and HSQC pulse sequences. Attempts to obtain similar complexes from the butadiynyl and hexatriynyl complexes Cl(dppe)$_2$Ru−(C≡C)$_n$H (n = 2, 3) gave, however, only intractable mixtures.

Electrochemistry in the CH_2Cl_2/NBu_4PF_6 (0.1 M) supporting electrolyte revealed stepwise oxidations of complexes **1a**,**b** in two fully reversible one-electron processes (Figure 1). Half-wave potentials are provided in Table 1 along with those of their symmetrically substituted bis(ethynyl)- and bis(vinyl)-substituted counterparts **4** and **5** and those of their protected and deprotected alkynyl precursors **3a** and **2a**,**b**. Comparison of the half-wave potentials of the pairs of complexes **1a**,**b** or **2a**,**b** shows that chloro by phenylacetylide substitution exerts only a small influence on the redox potentials, as is expected on the basis of their rather similar electrochemical ligand parameters P_L of −1.19 (Cl$^-$) and −1.22 (PhC≡C$^-$).[33,34] Comparison of **1a**,**b** with the symmetrically substituted complexes **4** and **5** reveals a clear dependence of the redox potential of the one organometallic subunit on the identity of the other. Thus, the potential of the first oxidation of **1a**,**b** is higher than that that in {Cl(dppe)$_2$Ru}$_2$(μ-C≡C-1,4-C$_6$H$_4$−C≡C) (**4**), while that for the second oxidation is lower than in {(P^{i}Pr$_3$)$_2$(CO)ClRu}$_2$(μ-CH=CH-1,4-C$_6$H$_4$−CH=CH) (**5**). A comparison of the half-wave potential of the mononuclear styryl complex (PhCH=CH)RuCl(CO)(P^{i}Pr$_3$)$_2$ ($E_{1/2}$ = +0.28 V) with the second oxidation potentials of **1a**,**b** (+0.140 and +0.155 V, respectively) further suggests that electron donation from the C≡C−RuCl(dppe)$_2$ "substituent" and further extension of the ligand's π-system overcompensate for the effects of electron loss from one-electron oxidation.[31] The potential separation between the individual half-wave potentials of ca. 360 mV is, however, nearly identical to that in **4** and appreciably larger than in **5**. The reader should note here that the redox-splitting of **1a**,**b** is not an adequate measure for electron delocalization in the radical cations due to the mainly ligand-centered redox processes and the differing organometallic end groups. The likewise unsymmetrically substituted Cp*(dppe)Fe−C≡C−1,4-C$_6$H$_4$−C≡C−Ru(dppe)$_2$Cl with $E_{1/2}$ values of −0.70 V ("Fe$^{II/III}$") and +0.05 V ("Ru$^{II/III}$") may serve as a further point of reference.[18] The mutual influence of each of the individual metal organic end groups on the thermodynamic stabilities of **1a**,**b** in their various oxidation states suggests a fair deal of orbital mixing within the entire {Ru}−C≡C−1,4-C$_6$H$_4$−CH=CH−{Ru′} entity.

Table 1. Half-Wave Potentials of Enynyl Complexes 1a,b, Symmetrically Bridged 4 and 5, and the Alkynyl Precursors 2a,b and 3a

	$E_{1/2}^{0/+}$ [V][a]	$E_{1/2}^{+/2+}$ [V]	$\Delta E_{1/2}$ [V][b]	K_c[c]
1a	−0.22	+0.14	0.36	1.2×10^6
1b	−0.195	+0.155	0.35	8.3×10^5
4	−0.33	+0.01	0.34	5.6×10^5
5	−0.075	+0.175	0.25	1.7×10^4
2a	0.035			
2b	−0.015			
3a	0.025			

[a] Potentials measured in CH_2Cl_2/NBu_4PF_6 (0.1 M); potentials are referenced to the $Cp_2Fe^{0/+}$ couple as an internal reference. [b] Difference between half-wave potentials. [c] Comproportionation constant for the reaction $A^{2+} + A \leftrightarrows 2A^{\bullet+}$ as calculated by the expression $K_c = \exp\{F\Delta E_{1/2}/(RT)\}$.

Owing to the rather substantial splitting of individual redox potentials, the intermediate, monooxidized radical cations **1a**$^{\bullet+}$ and **1b**$^{\bullet+}$ constitute thermodynamically stable species with comproportionation constants, K_c, of about 1×10^6 (Table 1). They could thus be generated by electrolysis inside a thin-layer electrolysis cell at a potential past the 0/+ wave as ruby to purple-red species and were characterized by their specific IR, UV/vis/NIR, and EPR signatures. Gratifyingly, **1a**,**b** possess the charge sensitive ν(C≡O) IR label at the vinyl ruthenium subunit, as well as ν(C≡C) and the various combinations of C−H bending and C=C stretching modes of the 1,4-(ethynyl)(vinyl)phenylene subunit. These labels are indicative of how oxidation affects the charge densities at the vinyl metal terminus and the bridge. IR data for the complexes **1a**,**b** in their various oxidation states are compiled in Table 2 and compared to those of symmetrical **4**$^{n+}$ and **5**$^{n+}$ (n = 0, 1, or 2). Of note are a substantial bleaching and a slight red shift by 4 cm^{-1} of the ν(C≡C) band at 2065 cm^{-1} of **1a** along with the emergence of a new C≡C band at 1967 cm^{-1} and a blue shift of the Ru(CO) band by 19 cm^{-1} during the first oxidation process. Another striking feature is the growth of intense phenylene-based absorptions in the 1580 to 1490 cm^{-1} range and of a band at 1157 cm^{-1} (Figures 2 and S1 of the Supporting Information). Similar observations have been reported for the radical cations of the symmetrical diethynyl and the divinyl phenylene-bridged complexes **4** and **5** and are a token of the strong participation of the bridge to the overall oxidation process.[9,22,24] Most

(33) Pombeiro, A. J. L. *New J. Chem.* **1997**, *21*, 649–660.
(34) Pombeiro, A. J. L. *Eur. J. Inorg. Chem.* **2007**, 1473–1482.

Table 2. Characteristic IR Data for Complexes 1a,b, 4, 5, 2a,b, and 3a in Their Various Oxidation States (1,2-$C_2H_4Cl_2$/NBu_4PF_6 (0.2 M))

	ν(C≡C)	ν(C≡O)	aryl[a]
1a	2065(m)	1910(s)	1565(m), 1527(w), 1497(w), 1486(m), 1482(s)
1a$^{\bullet+}$	2061(w), 1967(m)	1929(vs)	1581(m), 1559(m), 1521(m), 1513(m), 1493(s), 1483(m), 1157(vs)
1a^{2+}	1888(m)	1977(s)	1586(w), 1576(w), 1560(w)
1b	2059(s), 1981(w)	1910(s)	1591(w), 1563(w), 1528(w)
1b$^{\bullet+}$	2054(w), 1973(m)	1927(vs)	1579(s), 1524(s), 1512(s), 1492(vs), 1155(vs)
1b^{2+}	2047(m), 1900(m)	1974(m)	
4	2071(m)		
4$^{\bullet+}$	2068(w), 1966(s)		
4^{2+}	1918(m)		
5		1910	1573(m), 1561(m)
5$^{\bullet+}$		1932[b]	1519(m), 1503(s), 1481(s)
5^{2+}		1991	
2a	2067(s), 2038(w), 1968(m)		1577(s)
2a$^{\bullet+}$	1901(s)		1595(m)
3a	2149(m), 2065(s)		1573(s)
3a$^{\bullet+}$	1905(s)		1594(m), 1166(m)

[a] Combinations of C=C stretching and CH-bending modes. [b] Data for the "delocalized conformer".

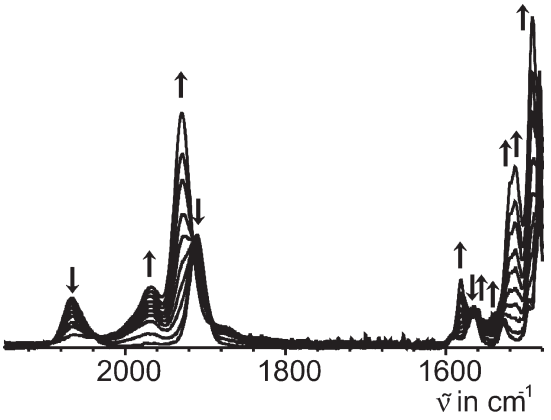

Figure 2. IR spectroscopic changes during the first oxidation of complex **1a** (**1a** → **1a**$^{\bullet+}$, 1,2-$C_2H_4Cl_2$/NBu_4PF_6, rt).

importantly, the ν(C≡C) bands of **1a**$^{\bullet+}$ appear at almost the same positions as in **4**$^{\bullet+}$, while ν(C≡O) of **1a**$^{\bullet+}$ is likewise close to its position in **5**$^{\bullet+}$. From this we conclude that both different ruthenium sites in **1a**$^{\bullet+}$ have about the same charge densities as in their symmetrical counterparts **4**$^{\bullet+}$ and **5**$^{\bullet+}$. Since these latter radical cations have both been found to be strongly delocalized systems, this must also be the case for **1a**$^{\bullet+}$. We are thus dealing with a bridge-centered radical cation with a fraction of the unipositive charge almost evenly delocalized over two different organometallic end groups. The same obviously holds for **1b**$^{\bullet+}$. Oxidized alkynyl precursors **2a**,**b**$^{\bullet+}$ have just one ν(C≡C) band at ca. 1900 cm^{-1} and thus at much lower energies than for **1a**,**b**$^{\bullet+}$ (Figures S2 and S3 of the Supporting Information).

More evidence toward full delocalization comes from the electronic spectra. Radical cations **4**$^{\bullet+}$ and **5**$^{\bullet+}$ present rather sharp and intense low-energy absorption bands. These have been assigned as the SOMO−*n* → SOMO transitions within an extended open-shell organometallic chromophore involving some charge transfer from the metal end groups to the central arene part of the bridge.[11,24] The close resemblance of those features to those of oxidized purely organic counterparts[35,36] has already been commented on.[24] Similar bands of identical appearance and like origin are observed in **1a**,**b**$^{\bullet+}$ at energies intermediate between those of the bordering symmetrical complexes (Table 3, Figures 3 and S4 of the Supporting Information). The distinct red shift of the band at lowest energy upon replacing the *trans*-chloro by the *trans*-phenylacetylide ligand shows that the organometallic π-system of **1a**,**b**$^{n+}$ extends over the entire (X)−Ru−C≡C−1,4-C_6H_4−CH=CH−Ru unit. Similar "radical" bands of the oxidized ruthenium alkynyl precursors **2a**,**b**$^{\bullet+}$ and **3a**$^{\bullet+}$ are less intense and appear at higher energies. As was found for the dinuclear complexes, replacement of the chloride by the phenylacetylide co-ligand produces a distinct red shift (Figures S5 and S6 of the Supporting Information).

Table 3. UV/Vis/NIR Data for Complexes 1a,b, 4,[9] 5,[24] 2a,b, and 3a in Their Various Oxidation States 1,2-$C_2H_4Cl_2$/NBu_4PF_6 (0.2 M)

	λ_{max} [nm] (energy in cm^{-1}; extinction coefficient [$M^{-1}\cdot cm^{-1}$])
1a	251 (39 840; 44 700), 368 (27 174; 32 500)
1a$^{\bullet+}$	264 (37 879; 41 000), 525 (19 048; 20 200), 1340 (7463; 33 000)
1a^{2+}	273 (36 630; 43 500), 400 (25 000; 6200), 719 (13 908; 35 700)
1b	364 (27 473; 33 000)
1b$^{\bullet+}$	535 (18 692; 12 500), 1491 (6707; 20 500)
1b^{2+}	408 (24 510; 7350), 633 (15 798; 12 400), 715 (13 986; 12 900), 835 (11 976; 13 300), 1024 (9766; 12 000)
2a	249 (40 161; 40 200), 362 (27 624; 22 800)
2a$^{\bullet+}$	270 (37 037; 43 200), 390 (25 641; 12 200), 615 (16 260; 2400), 861 (11 614; 9600), 1090 (9174; 1550)
2b	364 (27 473; 30 720)
2b$^{\bullet+}$	261 (38 314; 50 360), 301 (33 223; 25 190), 318 (31 447; 24 320), 342 (29 240; 18 980), 627 (15 949; 1620), 1157 (8643; 8010)
3a	254 (39 370; 40 010), 368 (27 174; 26 640)
3a$^{\bullet+}$	269 (37 175; 41 970), 407 (24 570; 17 380), 616 (16 234; 2360), 869 (11 507; 10 330)
4	245 (40 820; 9100), 276 (36 230; 3100), 370 (27 030; 4400),
4$^{\bullet+}$	268 (37 313; 2600), 490 (20 410; 2900), 535 (18 690; 3500), 1526 (6553; 3800)
4^{2+}	278 (35 970; 4500), 620 (16 130; 2100), 788 (12 690; 6000), 1170 (8547; 1000)
5	353 (28 329; 10 300), 405 (24 691; 2630), 503 (19 881; 1330)
5$^{\bullet+}$	346 (28 900; 10 300), 585 (17 095; 4270), 1255 (7968; 4110)
5^{2+}	266 (37594; 9060), 430 (23 256; 3230), 624 (16 026; 5360)

(35) Rauscher, U.; Bässler, H.; Bradley, D. D. C.; Hennecke, M. *Phys. Rev. B* **1990**, *42*, 9830–9836.
(36) Deussen, M.; Bässler, H. *Chem. Phys.* **1992**, *164*, 247–257.

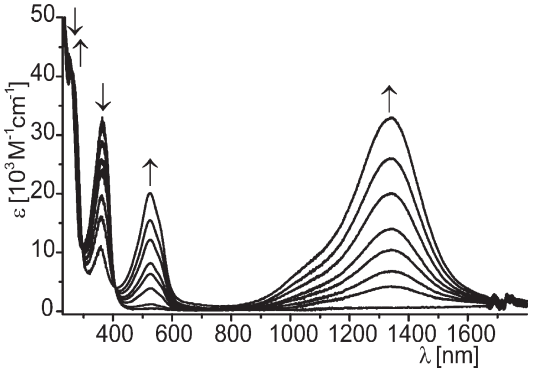

Figure 3. UV/vis/NIR spectroscopic changes during the first oxidation of complex **1a** (**1a** → **1a**$^{\bullet+}$, 1,2-$C_2H_4Cl_2$/NBu_4PF_6, rt).

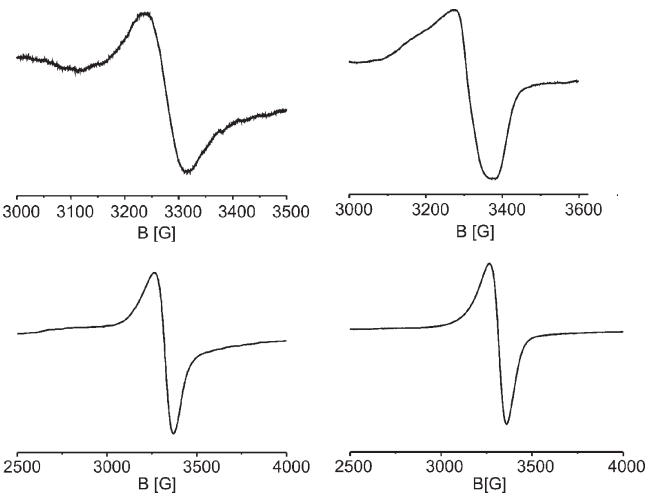

Figure 4. EPR spectra of chemically oxidized **1b**$^{\bullet+}$ in CH_2Cl_2 at rt (upper left) and at 107 K (upper right) and of **1a**$^{\bullet+}$ as a solid at rt (lower left) and at 107 K (lower right).

EPR spectroscopy is a powerful tool for elucidating the metal versus bridge character of a paramagnetic species. Genuine Ru(III) species are usually EPR inactive at room temperature due to rapid spin−lattice relaxation and exhibit axially or rhombically split *g*-tensors with large *g*-anisotropies at low temperatures as solids or frozen solutions and average *g*-values that differ strongly from the free electron value g_e of 2.0023. Paramagnetic ruthenium alkynyl complexes Cl(dppe)$_2$Ru−C≡C−C_6H_4-X-4$^{\bullet+}$[37] or Cp*(dppe)Ru−C≡C−C_6H_4-X-4$^{\bullet+}$[38] generally behave similarly with the exception of those with the most electron-releasing substituents X (X = NMe_2, NH_2, OMe), for which lower *g*-anisotropies at 80 K and isotropic signals in fluid solution were observed. In contrast, organic radicals typically give isotropic signals at room temperature and as solids or in frozen solution at *g*-values close to g_e. Complexes **4**$^{\bullet+}$[9] and **5**$^{\bullet+}$[24] are rare examples of oxidized organometallic ruthenium complexes that are EPR active in fluid solution and at room temperature.[31,37−39] Average *g*-values close to g_e and revealingly low (**4**$^{\bullet+}$) or altogether absent

(37) Paul, F.; Ellis, B. G.; Bruce, M. I.; Toupet, L.; Roisnel, T.; Costuas, K.; Halet, J.-F.; Lapinte, C. *Organometallics* **2006**, *25*, 649–665.
(38) Paul, F.; da Costa, G.; Bondon, A.; Gauthier, N.; Sinbandhit, S.; Toupet, L.; Costuas, K.; Halet, J.-F.; Lapinte, C. *Organometallics* **2007**, *26*, 874–896.
(39) Maurer, J.; Sarkar, B.; Zalis, S.; Winter, R. F. *J. Solid State Electrochem.* **2005**, *9*, 738–749.

Table 4. EPR Parameters of Chemically Oxidized 1a$^{\bullet+}$ and 1b$^{\bullet+}$ under Various Conditions

		T = rt	T = 103 K
1a$^{\bullet+}$	solution	no signal	2.0191
	solid	2.0289	2.0327
1b$^{\bullet+}$	solution	2.0568	$g_\perp$ = 2.1290, $g_\parallel$ = 2.0176, $\langle g_{av}\rangle$ = 2.0554[a]
	solid	2.0365	2.0383

[a] Data based on the spectrum simulation.[44]

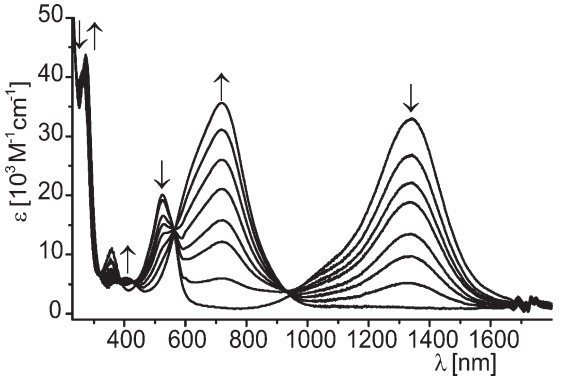

Figure 5. UV/vis/NIR spectroscopic changes during the second oxidation of complex **1a** (**1a**$^{\bullet+}$ → **1a**$^{2+}$, 1,2-$C_2H_4Cl_2$/NBu_4PF_6, rt).

(**5**$^{\bullet+}$) *g*-anisotropies in frozen solution evidence their dominant organic character with the major spin densities on the bridging ligand. Radical cations **1a**,**b**$^{\bullet+}$ were obtained by chemical oxidation with one equivalent of ferrocenium hexafluorophosphate. Solid samples of **1a**,**b**$^{\bullet+}$ provided strong isotropic signals at room temperature with *g*-values intermediate between those of **4**$^{\bullet+}$ and **5**$^{\bullet+}$ (Figures 4 and S7, S8 of the Supporting Information, Table 4). At 103 K the spectrum of **1a**$^{\bullet+}$ still remained isotropic, while simulations of the broader signal of **1b**$^{\bullet+}$ indicated an axial splitting (Table 4). Slightly different values were measured for their CH_2Cl_2/NBu_4PF_6 solutions, where only **1b**$^{\bullet+}$ proved to be EPR active at rt.

In keeping with the idea of full delocalization, dioxidized species **1a**,**b**$^{2+}$ display their Ru(CO) band at lower energy as in the divinylphenylene-bridged **5**$^{2+}$. This may be ascribed to the higher electron density at the (X)(dppe)$_2$Ru$^{\delta+}$ moiety compared to the Cl(CO)(P^{i}Pr$_3$)$_2$Ru$^{\delta'+}$ one at the opposite end, where δ and δ' symbolize the fractions of a unit charge at the respective ruthenium co-ligand entities. Moreover, the visible spectrum of **1a**$^{2+}$ features a prominent absorption band at an energy that is again intermediate between those of similar bands of **4**$^{2+}$ and **5**$^{2+}$ (Figure 5). As a curiosity, we note that the dioxidized phenylacetylide complex **1b**$^{2+}$ has a series of overlapping bands in its visible spectrum, leading to plateau-like absorption over the range 625 to 1050 nm (Figure 6, Table 3), which may indicate transitions from a larger manifold of lower-lying occupied donor orbitals spreading over the entire Ph−C≡C−Ru−C≡CAr′ unit into the emptied bridge-based, delocalized frontier orbital (the HOMO of neutral **1b**). The lower energy component at 9900 cm^{-1} is at much lower energy than that in **1a**$^{2+}$ (13 900 cm^{-1}).

In conclusion, we have found that the unsymmetrically bridged (X)(dppe)$_2$Ru−C≡C−1,4-C_6H_4−CH=CH−RuCl(CO)(P^{i}Pr$_3$)$_2$$^{\bullet+}$ (X = Cl, PhC≡C) complexes are bridge-centered radical cations featuring an extended X−Ru−C≡C−1,4-C_6H_4−CH=CH−Ru organometallic π-system

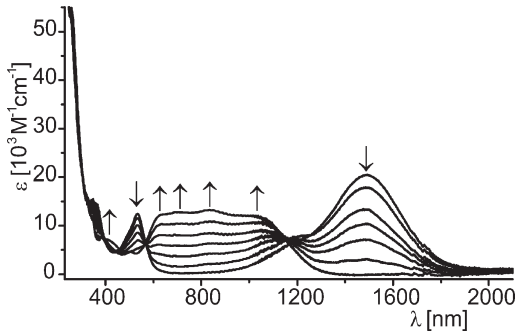

Figure 6. UV/vis/NIR spectroscopic changes during the second oxidation of complex **1b** (**1b**$^{\bullet+}$ → **1b**$^{2+}$, 1,2-$C_2H_4Cl_2$/NBu_4PF_6, rt).

with the same charge densities on the Ru−C≡C and Ru−CH=CH termini as in their symmetrical counterparts **4**$^{\bullet+}$ and **5**$^{\bullet+}$. This suggests that such (ethynyl)(vinyl)phenylene bridging motifs are as efficient as the bis(ethynyl) or bis(vinyl)phenylene ones at effecting charge and spin delocalization over long distances. Tuning of the extension of the organometallic π-chromophore and of the redox asymmetry within these complexes by varying the X substituent *trans* to the ethynyl group or the composition of the $Ru(PR_3)_2(CO)Y$ (Y = anionic ligand) moiety seems possible. The availability of *trans*-$(HC{\equiv}C{-}C_6H_4{-}C{\equiv}C)_2Ru(dppe)_2$ and the ease of further modification at the vinyl ruthenium moieties suggest that it is possible to create more extended systems with even stronger bridge participation to the "redox orbitals" (and thus enhanced delocalization),[40−42] as is the case for the pure alkynyl-bridged systems. Both of these issues are presently being explored in our laboratories.

Experimental Section

All manipulations were performed by standard Schlenk techniques under an argon atmosphere. Solvents were dried by standard procedures and degassed by saturation with argon prior to use. Infrared spectra were obtained on a Perkin-Elmer Paragon 1000 PC FT-IR instrument. ^{1}H (250.13 MHz), ^{13}C (62.90 MHz), and ^{31}P NMR spectra (101.26 MHz) were recorded on a Bruker AC 250 spectrometer as $CDCl_3$ or CD_2Cl_2 solutions at 303 K. The spectra were referenced to the residual protonated solvent (^{1}H), the solvent signal itself (^{13}C), or external H_3PO_4 (^{31}P). The assignment of ^{13}C NMR signals was aided by HSQC and HMBC experiments. UV/vis spectra were obtained on an Omega 10 spectrometer from Bruins Instruments in HELLMA quartz cuvettes with 1 cm optical path lengths. Elemental analyses (C, H, N) were performed at in-house facilities. The equipment for voltammetric and spectroelectrochemical studies and the conditions employed in this work were as described elsewhere.[43] Electron paramagnetic resonance (EPR) studies were performed on a tabletop X-band spectrometer Miniscope from Magnettech. Simulation of the spectrum of **1b**$^{\bullet+}$ in frozen CH_2Cl_2/NBu_4PF_6 solution was done with the EasySpin software package.[44]

Complexes *trans*-$Cl(dppe)_2Ru{-}CC{-}p{-}C_6H_4{-}CC{-}SiMe_3$ (**3a**), *trans*-$Cl(dppe)_2Ru{-}CC{-}p{-}C_6H_4{-}CC{-}H$ (**2a**), *trans*-$Ph{-}CC{-}Ru(dppe)_2{-}CC{-}p{-}C_6H_4{-}CC{-}SiMe_3$ (**3b**), and *trans*-$Ph{-}CC{-}Ru(dppe)_2{-}CC{-}p{-}C_6H_4{-}CC{-}H$ (**2b**) were prepared as previously reported[12,27]

***trans*-{Cl(dppe)$_2$Ru}(μ-C≡C−C$_6$H$_4$−CH=CH){RuCl(CO)(P^{i}Pr$_3$)$_2$} (1a).** CH_2Cl_2 (20 mL) was slowly added to a mixture of $RuHCl(CO)(P^iPr_3)_2$ (20.8 mg, 0.043 mmol) and $Ru(dppe)_2Cl(CC{-}1,4{-}C_6H_4{-}CCH)$ (**2a**) (45.4 mg, 0.043 mmol). After the red solution was stirred for 20 min the solvent was removed under reduced pressure. The rose-colored product was washed twice with *n*-hexane and dried under vacuum. Yield: 63.8 mg (97%). ^{1}H NMR (400 MHz, CD_2Cl_2): δ 8.39 (d, ^3J(H,H) = 13.3 Hz, 1H, RuC*H*=CH), 7.50−7.45 (m, 8H, *o*-C_6H_5 (dppe)), 7.36−7.30 (m, 8H, *o*-C_6H_5 (dppe)), 7.25−7.17 (m, 8H, *p*-C_6H_5 (dppe)), 7.03 (t, ^3J(H,H) = 7.68 Hz, 8H, *m*-C_6H_5 (dppe)), 6.96 (t, ^3J(H,H) = 7.68 Hz, 8H, *m*-C_6H_5 (dppe)), 6.81 (d, ^3J(H,H) = 8.1 Hz, 2H, *m*-H/Ru−C≡C−C_6H_4−), 6.55 (d, ^3J(H,H) = 8.1 Hz, 2H, *o*-H/Ru−C≡C−C_6H_4−), 5.93 (d, ^3J(H,H) = 13.3 Hz, 1H, RuC=C*H*), 2.82−2.74 (m, 6H, PC*H*CH_3), 2.68 (s, 8H, PCH_2CH_2P), 1.36−1.28 (m, 36H, PCHC*H*$_3$). ^{13}C{^{1}H} NMR (100 MHz, CD_2Cl_2): δ 203.0 (t, ^2J(C,P) = 12.8 Hz, C=O), 148.0 (t, ^2J(C,P) = 10.5 Hz, Ru*C*H=CH), 136.9 (m, *ipso*-C_6H_5 (dppe)), 136.0 (m, *ipso*-C_6H_5 (dppe)), 134.5 (m, *o*-C_6H_5 (dppe)), 134.4 (m, RuCH=*C*H), 134.2 (m, *o*-C_6H_5 (dppe)), 134.0 (s, *p*-C/Ru−C≡C−C_6H_4−), 130.0 (s, *o*-C/Ru−C≡C−C_6H_4−), 128.8 (s, *p*-C_6H_5 (dppe)), 128.7 (s, *p*-C_6H_5 (dppe)), 127.1 (m, *m*-C_6H_5 (dppe)), 126.9 (m, *m*-C_6H_5 (dppe)), 126.1 (m, *ipso*-C/Ru−C≡C−C_6H_4−), 123.2 (s, *m*-C/Ru−C≡C−C_6H_4−), 113.6 (s, Ru−C≡*C*), 31.87 (m, [^1J(P,C) + ^3J(P,C)] = 23 Hz, PCH_2CH_2P), 24.3 (vt, *J*(C,P) = 9.7 Hz, P*C*HCH$_3$), 19.89 and 19.87 (both s, PCH*C*H$_3$); the signal for Ru*C*C was not observed. ^{31}P NMR (400 MHz, CD_2Cl_2): δ 49.5 (s, dppe), 38.5 (s, P^{i}Pr$_3$). Anal. Calcd for $C_{81}H_{96}Cl_2P_6ORu_2$: C, 63.38; H, 6.25. Found: C, 62.97; H, 5.99.

***trans*-{(Ph−C≡C)(dppe)$_2$Ru}(μ-C≡C−C$_6$H$_4$−CH=CH){RuCl(CO)(P^{i}Pr$_3$)$_2$} (1b).** The synthesis of **1b** followed the procedure given for **1a**. From 10.3 mg of $RuHCl(CO)(P^iPr_3)_2$ (0.021 mmol) and 24.0 mg of $Ru(dppe)_2(CCC_6H_5)(CC{-}1,4{-}C_6H_4{-}CCH)$ (**2b**) (0.021 mmol) **1b** was obtained as a rose-colored solid. Yield: 33.0 mg (95%). ^{1}H NMR (400 MHz, CD_2Cl_2): δ 8.41 (d, ^3J(H,H) = 13.3 Hz, 1H, RuC*H*=CH), 7.61−7.54 (m, 8H, *o*-C_6H_5 (dppe)), 7.52−7.45 (m, 8H, *o*-C_6H_5 (dppe)), 7.23−7.15 (m, 8H, *p*-C_6H_5 (dppe)), 7.15−7.10 (m, 2H, *m*-C_6H_5 (C≡C−C_6H_5), 7.03−6.92 (m, 17H, *m*-C_6H_5 (dppe) and *p*-C_6H_5 (C≡C−C_6H_5), 6.85 (d, ^3J(H,H) = 8.1 Hz, 2H, *m*-H/Ru−C≡C−C_6H_4−), 6.76 (d, ^3J(H,H) = 7.4 Hz, 2H, *o*-C_6H_5 (C≡C−C_6H_5), 6.67 (d, ^3J = 8.1 Hz, 2H, *o*-H/Ru−C≡C−C_6H_4−), 5.95 (d, ^3J(H,H) = 13.3 Hz, 1H, RuCH=C*H*), 2.85−2.73 (m, 6H, PC*H*CH), 2.64 (s, 8H, PCH_2CH_2P), 1.39−1.27 (m, 36H, PCHC*H*$_3$). ^{13}C{^{1}H} NMR (100 MHz, CD_2Cl_2): δ 203.5 (t, ^2J(C,P) = 13.1 Hz, C=O), 148.4 (t, ^2J(C,P) = 11.0 Hz, Ru*C*H=CH), 138.1−137.4 (m, *ipso*-C_6H_5 (dppe)), 134.9 (t, ^3J(C,P) = 3.5 Hz, RuCH=*C*H), 134.7 (m, *J*(C,P) = 2.4 Hz, *o*-C_6H_5 (dppe)), 134.6 (m, *J*(C,P) = 2.4 Hz, *o*-C_6H_5 (dppe)), 134.4 (t, ^4J(C,P) = 2.33 Hz, *p*-C/Ru−C≡C−C_6H_4−), 131.1 (m, *ipso*-C_6H_5 (C≡C−C_6H_5)), 130.3 (s, *o*-C/Ru−C≡C−C_6H_4−), 130.2 (s, *o*-C_6H_5 (C≡C−C_6H_5)), 129.0 (s, *p*-C_6H_5 (dppe)), 128.9 (s, *p*-C_6H_5 (dppe)), 127.8 (s, *m*-C_6H_5 (C≡C−C_6H_5)), 127.5−127.3 (m, *m*-C_6H_5 (dppe)), 126.6 (m, *ipso*-C/Ru−C≡C−C_6H_4−), 123.7 (s, *m*-C (Ru−C≡C−C_6H_4−)), 123.1 (s, *p*-C_6H_5 (C≡C−C_6H_5)), 117.4 (s, Ru−C≡*C*−C_6H_4−), 116.7 (s, Ru−C≡*C*-C_6H_5), 31.84 (m, [^1J(P,C) + ^3J(P,C)] = 23 Hz, PCH_2CH_2P), 24.80 (vt, *J*(P,C) = 9.7 Hz, P*C*HCH$_3$), 20.13, 19.92 (both s, PCH*C*H$_3$). ^{31}P NMR (400 MHz, CD_2Cl_2): δ 53.8 (s, dppe), 38.5 (s, P^{i}Pr$_3$). Anal. Calcd for $C_{89}H_{101}ClP_6ORu_2$: C, 66.39; H, 6.32. Found: C, 66.01; H, 6.14.

{RuCl(CO)(P^{i}Pr$_3$)$_2$}$_2$(μ-CH=CH−C$_6$H$_4$−CH=CH) (5). ^{13}C{^{1}H} NMR (100 MHz, CD_2Cl_2): 203.4 (t, ^2J(P,C) = 12.5 Hz, CO), 148.5 (t, ^2J(C,P) = 11.4 Hz, Ru*C*H=CH), 135.3 (t, ^4J(P,C) = 1.9 Hz, *ipso*-C/C_6H_4), 134.5 (t, ^3J(P,C) = 3.8 Hz, RuC=*C*H), 124.4

(40) Rigaut, S.; Olivier, C.; Costuas, K.; Choua, S.; Fadhel, O.; Massue, J.; Turek, P.; Saillard, J.-Y.; Dixneuf, P. H.; Touchard, D. *J. Am. Chem. Soc.* **2006**, *128*, 5859–5876.

(41) Olivier, C.; Costuas, K.; Choua, S.; Maurel, V.; Turek, P.; Saillard, J.-Y.; Touchard, D.; Rigaut, S. *J. Am. Chem. Soc.* **2010**, *132*, 5638–5651.

(42) Xi, B.; Xu, G.-L.; Fanwick, P. E.; Ren, T. *Organometallics* **2009**, *28*, 2338–2341.

(43) Winter, R. F.; Klinkhammer, K.-W.; Zális, S. *Organometallics* **2001**, *20*, 1317–1333.

(44) Stoll, S.; Schweiger, A. *J. Magn. Reson.* **2006**, *178*, 42–55.

(s, CH/C_6H_4), 24.76 (t, $^1J(P,C) = 9.83$ Hz, $PCHCH_3$), 20.08, 19.85 (both s, $PCHCH_3$).

Acknowledgment. We gratefully acknowledge support of this work by Deutsche Forschungsgemeinschaft (grant Wi 1272/7-2), the Bayerisch-Französisches Hochschulzentrum (BFHZ), and the German French intergovernmental S&T cooperation programs PROCOPE (DAAD/Egide) and the Region Bretagne (E.D.P. grant). We also wish to thank the students Roman Sommer and Andreas Gross for recording the EPR spectra.

Supporting Information Available: This material is available free of charge via the Internet at http://pubs.acs.org.